

# Synthesis and characterization of Fe<sub>2</sub>O<sub>3</sub> containing aluminas by thermal decomposition of modified ammonium dawsonite

Irene Pitsch,<sup>\*a</sup> Wolfgang Geßner,<sup>a</sup> Angelika Brückner,<sup>a</sup> Hartmut Mehner,<sup>b</sup> Steffen Möhmel,<sup>a</sup> Doris-Christine Uecker<sup>a</sup> and Marga-Martina Pohl<sup>a</sup>

<sup>a</sup>Institut für Angewandte Chemie Berlin-Adlershof e. V., Richard-Willstätter-Str.12, Berlin 12484, Germany

<sup>b</sup>Bundesanstalt für Materialforschung/Prüfung, Richard-Willstätter-Str.11, Berlin 12484, Germany

Received 14th February 2001, Accepted 18th June 2001  
First published as an Advance Article on the web 22nd August 2001

Aluminas with Fe<sub>2</sub>O<sub>3</sub> particles finely divided in the Al<sub>2</sub>O<sub>3</sub> matrix were prepared *via* a crystalline precursor derived from ammonium dawsonite and its calcination. The precursors with Fe content between 1 and 10 wt% were synthesized by reaction of ammonium hydrogen carbonate with mixtures containing aluminium ammonium sulfate and ferric ammonium sulfate. The characterization of the as-synthesized and calcined products by chemical analysis, XRD, EPR, Mössbauer, TEM and adsorption measurements shows that all the Fe<sup>3+</sup> ions are incorporated into the structure of dawsonite when the Fe content is low and that the calcined materials with micropores and mesopores (maximum 30–40 Å) also contain very small Fe<sub>2</sub>O<sub>3</sub> particles (<10 nm) at higher Fe contents.

Fe<sub>2</sub>O<sub>3</sub>-containing aluminas are interesting materials for catalytic applications and for preparing nanocomposites and coatings. In special fields of catalysis *e.g.* in the selective reduction of nitrogen monoxide with hydrocarbons<sup>1</sup> or in the selective hydrogenation of sulfur dioxide to elemental sulfur<sup>2</sup> it is necessary to create small particles of iron oxide in the Al<sub>2</sub>O<sub>3</sub> matrix and surface, respectively, to enhance the catalytic activity. The particle size strongly depends on the support used and preparation method. Therefore many articles in the literature deal with the nature of the iron oxide species formed by the interaction between the metal oxide and the support.<sup>3–5</sup>

High-purity aluminas for industrial applications can be synthesized by thermal decomposition of ammonium aluminium carbonate dihydroxide [NH<sub>4</sub>Al(OH)<sub>2</sub>CO<sub>3</sub>; ammonium dawsonite] giving a fine ceramic raw material<sup>6</sup> and catalyst support.<sup>7</sup> By varying the synthesis conditions given in the literature<sup>8</sup> by introducing ferric [iron(III)] cations into the synthesis mixtures, Fe-doped Al<sub>2</sub>O<sub>3</sub> materials should be obtained.

Here we describe this new synthesis route to prepare aluminas with finely divided Fe<sub>2</sub>O<sub>3</sub> particles in the Al<sub>2</sub>O<sub>3</sub> matrix *via* a crystalline precursor derived from ammonium dawsonite and its calcination. The precursor preparation consists of the reaction of ammonium hydrogen carbonate with a mixture of ammonium aluminium sulfate and ammonium iron sulfate. Characteristic data of the as-synthesized and calcined products are also given.

## Experimental

### Sample preparation

Samples of Fe-doped ammonium dawsonite [NH<sub>4</sub>Al(OH)<sub>2</sub>CO<sub>3</sub>] with Fe contents in the range between 1 and 10 wt% (relative to Al<sub>2</sub>O<sub>3</sub>) were prepared by reaction of ammonium hydrogen carbonate (2 M) in water with an aqueous solution (0.1 M) containing aluminium ammonium sulfate [NH<sub>4</sub>Al(SO<sub>4</sub>)<sub>2</sub>·12H<sub>2</sub>O] and ferric ammonium sulfate [NH<sub>4</sub>Fe(SO<sub>4</sub>)<sub>2</sub>·12H<sub>2</sub>O] in an appropriate ratio. The aluminium

and iron compounds were added to the carbonate under stirring over a period of 2 h at 333 K. The resulting product was separated from the liquid by filtering. After washing free of sulfate the precipitate was dried at room temperature and then calcined in air at 873, 1073 and 1173 K for 4 h.

For comparison, Fe<sub>2</sub>O<sub>3</sub> containing alumina samples were also prepared by impregnation of a pure ammonium dawsonite dried at room temperature and a commercial alumina with an aqueous solution containing the appropriate amount of ferric nitrate. The samples are listed in Table 1.

### Instrumentation

Chemical analysis of the calcined materials was carried out using an inductively coupled plasma (ICP) spectrometer, Optima 3000 XL (Perkin Elmer).

X-Ray powder diffractograms were obtained by means of the URD 6 powder diffractometer (Freiberger Präzisionsmechanik GmbH) using Cu-K $\alpha$  radiation.

The nitrogen adsorption isotherms were measured using an automated gas adsorption system ASAP 2000M (Micromeritics). The surface area and pore diameter of the calcined materials were calculated by the BET<sup>9</sup> and BJH method.<sup>10</sup>

EPR spectra of the as-synthesized and calcined samples were recorded using a c.w. spectrometer ELEXSYS 500-10/12 (Bruker) at X-band at 77 and 293 K using a finger Dewar.

Mössbauer spectra for the samples (80–160 mg cm<sup>-2</sup>) were measured in transmission geometry using a 300 MBq Co-57 source in a Cr matrix. The spectra were registered in constant acceleration mode with a WissEl Mössbauer spectrometer (Starnberg, Germany) at room temperature with the aid of a proportional counter. Parameter fits (Table 3) were performed using a standard least-squares fitting routine. Under the assumption that the f-factors were equal for different iron sites and phases, the spectra areas were evaluated as a percentage of the total spectrum. Errors for isomer shift ( $\delta$ ) referred to metallic iron, quadrupole splitting ( $\Delta$ ) and the line width ( $\Gamma$ ) were 0.01 mm s<sup>-1</sup> and for most of the areas it was below 2%.

For TEM investigations a Philips CM 20 was used at 200 kV

**Table 1** Preparation, chemical composition and XRD results of pure ammonium dawsonite, Fe-doped samples and of their calcined products

Sample <sup>a</sup>	Wt% Fe	Modification method	Al/Fe ratio in starting mixture	Al/Fe ratio in calcined product (ICP)	Crystalline phases identified by XRD
0A 0A/600	0				Dawsonite Amorphous
1A 1A/600	1	Synthesis	109.5	98.2	Dawsonite Amorphous
3A 3A/600	3	Synthesis	33.5	32.9	Dawsonite Amorphous
3B/600	3	Impregnation of dawsonite	—	35.8	Amorphous, ( $\gamma$ -Al <sub>2</sub> O <sub>3</sub> )
3C/600	3	Impregnation of commercial alumina	—	n.d.	$\gamma$ -Al <sub>2</sub> O <sub>3</sub>
10A 10A/600	10	Synthesis	11.0	10.8	Dawsonite Amorphous

<sup>a</sup>The calcined samples are denoted by indicating the applied temperature in °C.

with a LaB<sub>6</sub> cathode. The samples were prepared by depositing them on a Lacey-carbon support without any pretreatment.

## Results and discussion

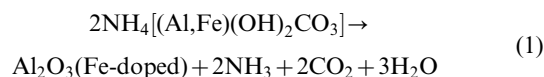
Reaction of ammonium hydrogen carbonate with aluminium ammonium sulfate led to the formation of a white precipitate. XRD investigation of this powdery precipitate dried at room temperature reveals the expected structure of ammonium dawsonite (sample 0A; XRD data file 42-250). After calcination at temperatures between 873 and 1173 K amorphous and crystalline transition aluminas, respectively, are obtained (Tables 1 and 2). The materials are porous and comprise micropores and mesopores depending on the applied thermal treatment. The pore size distribution of the materials calcined at 873 K for 4 h shows a relatively small pore size distribution in the range of mesopores (maximum 30–40 Å).<sup>11</sup> Fe<sup>3+</sup> ions were introduced into the precursor structure by adding [NH<sub>4</sub>Fe(SO<sub>4</sub>)<sub>2</sub>·12H<sub>2</sub>O] to the synthesis mixture. By mixing the starting components during the synthesis procedure no brown coloured precipitates were observed either for low iron contents (samples 1A and 3A) or in sample 10A with 10 wt% Fe. This suggests that the iron containing particles are finely divided within the resulting materials. After drying at room temperature white or nearly white (sample 10A) powdery solids are obtained.

**Table 2** Surface area, pore diameter and XRD results of calcined pure and Fe-doped ammonium dawsonites

Sample <sup>a</sup>	BET surface area/m <sup>2</sup> g <sup>-1</sup>	Average BJH pore diameter/Å (4V/O <sub>BJH</sub> )	Al <sub>2</sub> O <sub>3</sub> phases identified by XRD
0A/600	339	37	Amorphous
0A/800	147		$\gamma$ , $\delta$ , $\theta$
0A/900	106		$\gamma$ , $\delta$ , $\theta$
1A/600	376	34	Amorphous
1A/800	145	41	$\gamma$
3A/600	304	42	Amorphous, ( $\gamma$ )
3A/600†	263	38	Amorphous
3A/800†	136		Amorphous, $\gamma$
3A/900†	108	69	$\gamma$ , $\delta$ , $\theta$
3B/600	391	43	Amorphous, ( $\gamma$ )
3B/600†	425	40	$\gamma$ , amorphous
3B/800†	157		$\gamma$
3B/900†	123		$\gamma$ , $\delta$ , $\theta$
10A/600	222	49	Amorphous
10A/800	125	52	$\gamma$ , amorphous
10A/900	40	156	$\alpha$

<sup>a</sup>Samples denoted by † refer to a second synthesis run of samples 3A and 3B.

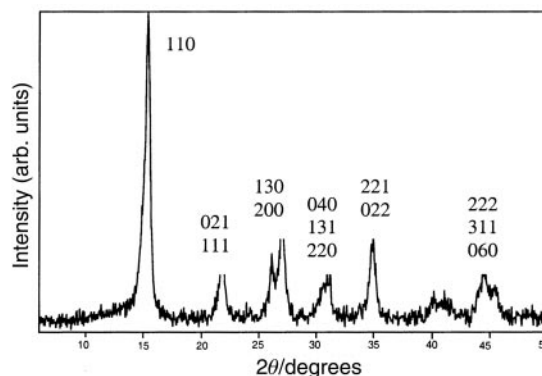
The X-ray diffraction pattern of the as-synthesized sample 10A with high Fe content (Fig. 1) is in accord with the data for crystalline ammonium dawsonite (XRD data file 42-250) and no peaks for iron containing phases are observed. During the thermal treatment at 873 K the Fe-doped ammonium dawsonite is completely converted into amorphous Al<sub>2</sub>O<sub>3</sub> material according to eqn. (1) (see also Table 1)



For sample 3B/600 (Table 1) prepared by impregnation of ammonium dawsonite with ferric nitrate and further calcination the predominantly amorphous and light brown material contains a small amount of  $\gamma$ -Al<sub>2</sub>O<sub>3</sub>.

To gain information on the surface and pore structure of the Fe-doped aluminas they were investigated by measuring their nitrogen adsorption isotherms. The resulting data are given in Table 2.

As an example Fig. 2 shows the isotherm of the sample 3A/600 which seems to be typical for these materials after calcination at 873 K. The course of the isotherm in the low-pressure branch suggests a material containing a small number of micropores. The increase in the high-pressure branch and the hysteresis loop also indicate the existence of mesopores. The pore size distributions of samples 3A/600 and 3A/900 are shown in Fig. 3. As can be seen the pore size distribution is in the range 30–40 Å and is relatively small. This shifts to higher sizes (maximum at 60 Å) with increasing calcination temperatures caused by a loss of micropores and also of part of the mesopores. The BET surfaces of the samples calcined at 873 K are different from each other and in the range 222–391 m<sup>2</sup> g<sup>-1</sup> (Table 2). An explanation for this observation may be the

**Fig. 1** X-Ray diffraction diagram of the as-synthesized sample 10A (10 wt% Fe).

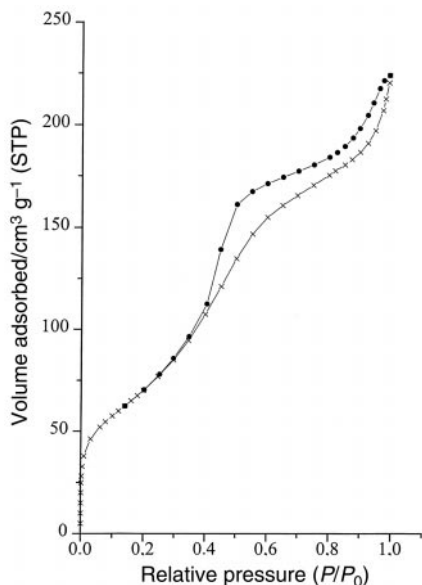


Fig. 2 77 K nitrogen isotherm of sample 3A/600†: (—×—) adsorption, (—●—) desorption.

amorphous character of the  $\text{Al}_2\text{O}_3$  materials. After calcination at higher temperatures aluminas consisting mainly of  $\gamma$ - and  $\delta$ -( $\delta$ - $\gamma$ -) $\text{Al}_2\text{O}_3$  are obtained with surfaces areas in the range  $125$ – $157 \text{ m}^2 \text{ g}^{-1}$  (1073 K) and  $106$ – $123 \text{ m}^2 \text{ g}^{-1}$  (1173 K), respectively. The sample 10A/900 seems to be an exception; the surface area is strongly decreased ( $40 \text{ m}^2 \text{ g}^{-1}$ ) and the pore size distribution shows a maximum at  $60 \text{ \AA}$  and additional pores greater than  $200 \text{ \AA}$ . The mesoporous character of the metastable transition in alumina is changed caused by its transformation into  $\alpha$ - $\text{Al}_2\text{O}_3$  (Table 2). This destabilizing effect of Fe dopants in aluminas is known and described in the literature.<sup>12</sup>

To get information regarding the nature and surroundings of the ferric cations in the as-synthesized samples and dependence on the synthesis conditions of the calcined samples EPR measurements have been performed. The EPR spectra of the as-synthesized samples are dominated by a line at an apparent  $g$ -value of  $g' = 4.3$  [Fig. 4(a)]. Such signals are known to originate from isolated  $\text{Fe}^{3+}$  ions with rhombic symmetry of the fine structure tensor when the zero field splitting is large in comparison to the Zeeman energy,<sup>13</sup> *i.e.*, when  $D \gg h\nu$  and  $E/D \approx 1/3$ . The coordination of such  $\text{Fe}^{3+}$  sites may be either distorted tetrahedral or octahedral. In the dawsonite structure it is very likely that such  $\text{Fe}^{3+}$  ions substitute for  $\text{Al}^{3+}$  ions in lattice positions, where they are coordinated by six oxide ions. The difference of the ionic radii of  $\text{Fe}^{3+}$  and  $\text{Al}^{3+}$  is assumed to be responsible for the distortion of the local coordination sphere giving rise to the rather large zero field splitting.

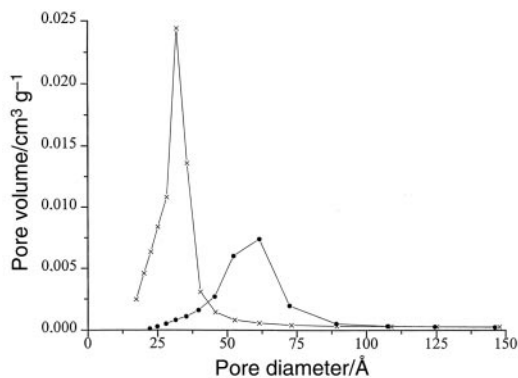


Fig. 3 Distribution of pore diameters: (—×—) sample 3A/600†, (—●—) sample 3A/900†.

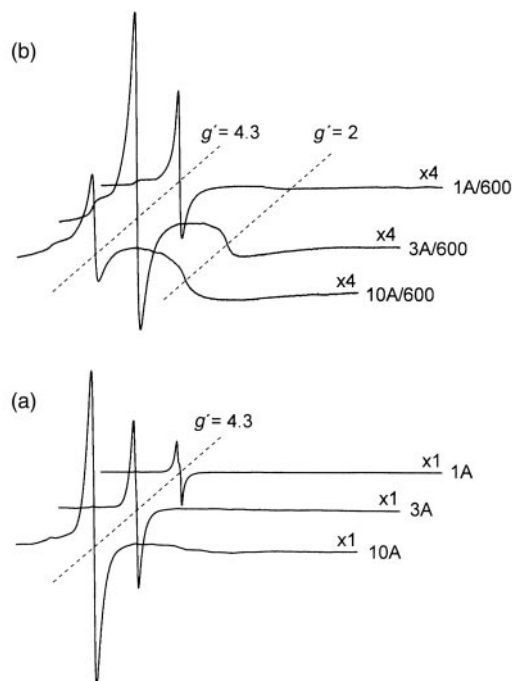


Fig. 4 EPR spectra of as-synthesized (a) and calcined (b) samples with different Fe contents, measured at 77 K.

Evidence for octahedral coordination is also provided by Mössbauer measurements discussed below. As expected, the amount of isomorphously substituted  $\text{Fe}^{3+}$  ions rises with increasing total iron content, but not in a linear manner. At low loadings (samples 1A and 3A) virtually all  $\text{Fe}^{3+}$  ions are located in lattice positions. This is obviously not the case for higher iron contents (sample 10A). The signal at  $g' = 4.3$  in sample 10A is only slightly stronger than in sample 3A and a very weak and broad line at  $g' = 2$  points to the formation of clusters of iron hydroxide.

Upon calcination at 873 K (sample 10A/600) more and larger  $\text{Fe}_2\text{O}_3$  clusters are formed [Fig. 4(b)]. This is evident from the enhanced intensity of the signal at  $g' = 2$  which is roughly the same at 77 K and at 293 K. This points to antiferromagnetic interaction between the  $\text{Fe}^{3+}$  ions within the clusters. In case of pure paramagnetic behaviour the line intensity at 77 K should be 3.8 times higher than at 293 K according to the Curie–Weiss law. The diminished intensity of the signal at  $g' = 4.3$  indicates that isomorphously substituted  $\text{Fe}^{3+}$  ions are released from the lattice and contribute to  $\text{Fe}_2\text{O}_3$  cluster formation. This is also evident, although to a lower extent, for sample 3A/600 while at low iron loadings (sample 1A/600) obviously all  $\text{Fe}^{3+}$  ions remain in Al lattice positions. Comparison of the EPR spectra in Fig. 4(b) suggests that the stability of  $\text{Fe}^{3+}$  ions in Al lattice sites of the calcined samples decreases when the total iron content exceeds a certain limit which appears to be between 3 and 10 wt%.

When a pure ammonium dawsonite or a commercial alumina are impregnated with an aqueous ferric nitrate solution and subsequently calcined at 873 K,  $\text{Fe}^{3+}$  ions are to a certain extent also incorporated into Al positions. This is evident from the signals at  $g' = 4.3$  in the EPR spectra of samples 3B/600 and 3C/600 (Fig. 5). However, it is interesting that in both cases the intensity of this signal and, thus, the number of isomorphously substituted  $\text{Fe}^{3+}$  ions is smaller than in sample 3A/600 prepared *via* synthesis. This indicates that the addition of  $\text{Fe}^{3+}$  ions during the crystallisation of the dawsonite precursor is a suitable method for obtaining aluminas with a high percentage of well isolated  $\text{Fe}^{3+}$  ions in lattice sites.

Further information on the structure of the iron species in as-synthesized and calcined samples has been obtained by

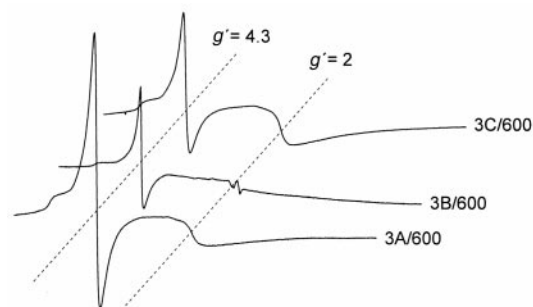


**Fig. 5** EPR spectra of calcined samples prepared *via* synthesis (3A/600) and *via* impregnation (3B/600, 3C/600), measured at 77 K.

Mössbauer measurements. The Mössbauer parameters are listed in Table 3. All isomer shifts are  $>0.3 \text{ mm s}^{-1}$  indicating that all  $\text{Fe}^{3+}$  sites are octahedrally coordinated.<sup>14</sup> The spectra of the as-synthesized samples 1A and 3A contain a broad singlet which is characteristic for  $\text{Fe}^{3+}$  ions in a fairly symmetric surrounding. In agreement with the EPR spectra, we attribute this signal to  $\text{Fe}^{3+}$  ions in Al sites of the dawsonite structure. The distortion of the coordination symmetry which is evidenced in the EPR spectra by the position of the signal at  $g' = 4.3$  might be the reason for the rather large line width of the Mössbauer signal [Fig. 6(a)] and can be explained by the unresolved quadrupole splitting.

After calcination, the Mössbauer spectrum of sample 1A/600 can still be fitted by one doublet indicating the presence of one type of Fe species most probably located in lattice sites. This corresponds well to the EPR results [Fig. 4(b)]. The observed quadrupole splitting,  $\Delta = 1.25 \text{ mm s}^{-1}$  (Table 3) suggests that the coordination symmetry of the  $\text{Fe}^{3+}$  ions is lowered. The iron is located in small oxidic particles and/or on Al positions in  $\text{Al}_2\text{O}_3$ .

To properly fit the Mössbauer spectrum of the calcined sample 3A/600 [Table 3, Fig. 6(b)] two doublets representing different types of  $\text{Fe}^{3+}$  species have to be superimposed. By comparing their relative intensities with those of the two signals in the respective EPR spectrum [Fig. 4(b)] we assign the doublet with  $\Delta = 1.39 \text{ mm s}^{-1}$  to isomorphously incorporated  $\text{Fe}^{3+}$  ions and the other to  $\text{Fe}^{3+}$  ions in oxidic clusters. This is also supported by the good agreement of the quadrupole splitting with the corresponding value in sample 1A/600 in

**Table 3** Mössbauer parameters of as-synthesized and calcined Fe-doped dawsonites:  $\delta$ =isomer shift,  $\Delta$ =quadrupole splitting,  $\Gamma$ =line width,  $I$ =relative signal area

Sample	Singlet			Doublet			
	$\delta/$ $\text{mm s}^{-1}$	$\Gamma/$ $\text{mm s}^{-1}$	$I$ (%)	$\delta/$ $\text{mm s}^{-1}$	$\Delta/$ $\text{mm s}^{-1}$	$\Gamma/$ $\text{mm s}^{-1}$	$I$ (%)
1A	0.32	1.20	100				
1A/600				0.31	1.25	1.16	100
3A	0.34	1.12	100				
3A/600				0.32	1.39	0.78	64
				0.32	0.88	0.57	37
3B/600				0.34	0.58	0.34	22
				0.34	0.89	0.33	29
				0.33	1.22	0.36	28
				0.32	1.65	0.46	20
10A	0.36	2.01	52	0.38	0.32	0.35	22
				0.34	0.48	0.43	26
10A/600				0.32	0.47	0.32	8
				0.33	0.79	0.35	25
				0.33	1.12	0.39	35
				0.32	1.50	0.41	24
				0.32	1.95	0.44	8

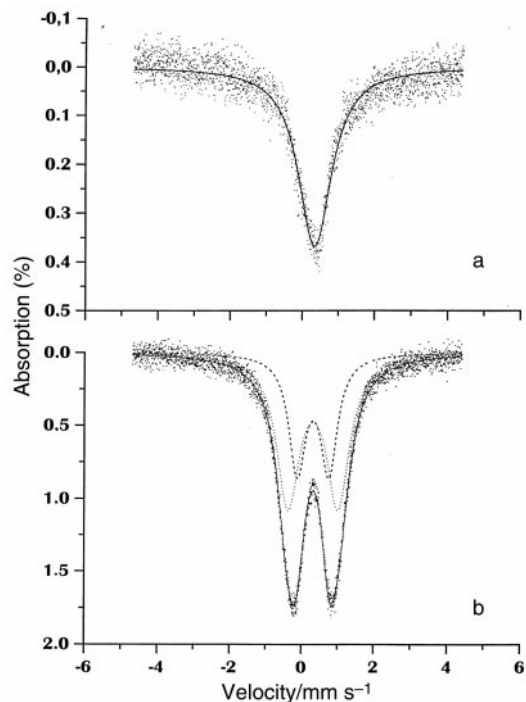


**Fig. 6** Room temperature Mössbauer spectra of the samples 3A (a) and 3A/600 (b).

which all iron ions are in lattice sites. By contrast, the Mössbauer spectrum of sample 3B/600 with 3 wt% Fe prepared by impregnation and subsequent calcination is fitted by at least four doublets (Fig. 7, Table 3). This points to a distribution of quadrupole split subspectra and the presence of strain effects in the iron coordination within the  $\text{Fe}_2\text{O}_3$  clusters is suggested by the very broad line width of the  $g' = 2$  signal in the EPR spectrum of Fig. 5.

The Mössbauer spectrum of the as-synthesized Fe rich sample 10A has to be fitted by at least one broad singlet and two doublets [Fig. 8(a), Table 3]. In agreement with the EPR spectrum, [Fig. 4(a)] this points to the presence of different Fe species in oxidic or hydroxidic clusters. The rather high number of doublets necessary to fit the experimental spectrum of the calcined sample [10A/600, Fig. 8(b)] suggests the local surrounding of the Fe sites in the oxidic clusters is different due to strain effects as discussed above also for sample 3B/600.

In the room-temperature spectra no magnetic sextet of  $\alpha\text{-Fe}_2\text{O}_3$  is observed. This indicates that the oxidic clusters in

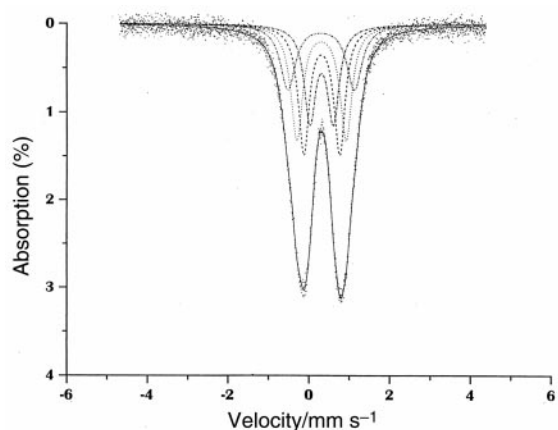


**Fig. 7** Room-temperature Mössbauer spectrum of sample 3B/600.

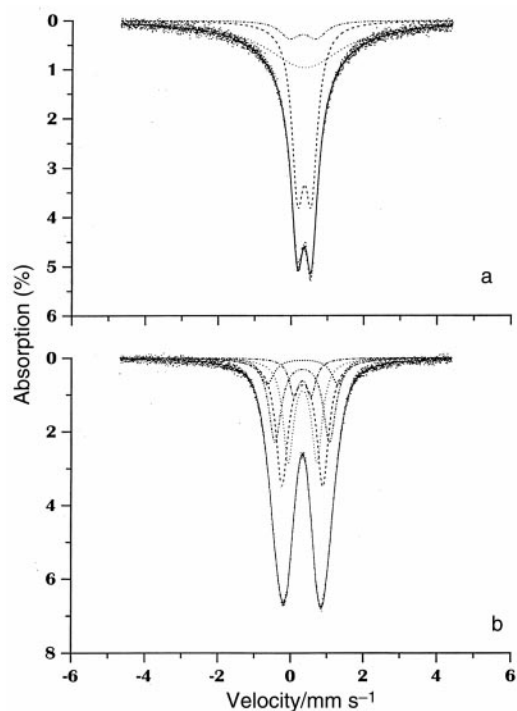


**Fig. 8** Room-temperature Mössbauer spectra of the samples 10A (a) and 10A/600 (b).

the calcined  $\text{Al}_2\text{O}_3$  material are finely divided superparamagnetic  $\text{Fe}_2\text{O}_3$  particles with diameters  $< 10$  nm.

No separate  $\text{Fe}_2\text{O}_3$  particles were observed in the TEM investigations of sample 10A/600 [Fig. 9(a)]; this confirms that they are very small. It was not possible to distinguish between the Al and Fe oxidic structures, respectively, existing in the nanometer range in the material under the applied experimental conditions. Therefore the particle diameter of ferric oxide must be also in this range and amounts to a few nanometers. In contrast, the  $\text{Fe}_2\text{O}_3$  particle diameters in samples obtained by impregnating and calcining commercial aluminas with ferric nitrate [sample 3C/600, Fig. 9(b)] were much larger (20–50 nm).

## Conclusions

Iron-containing ammonium dawsonite with Fe contents between 1 and 10 wt% can be synthesized by the reaction of ammonium hydrogen carbonate in water with an aqueous solution containing aluminium ammonium sulfate and ferric ammonium sulfate.

XRD investigations of the as-synthesized solids reveal the ammonium dawsonite structure  $[\text{NH}_4\text{Al}(\text{OH})_2\text{CO}_3]$ ; no peaks for iron containing phases are observed also after thermal treatment.

By means of adsorption measurements it is established that the calcined and amorphous materials contain micro- and mesopores. The pore size distribution of mesopores is relatively small and shifts to higher sizes after thermal treatment at higher temperatures.

EPR and Mössbauer results of the as-synthesized solids show that all the  $\text{Fe}^{3+}$  cations are incorporated into the structure of ammonium dawsonite when the Fe content is small (1–3 wt%). In the ammonium dawsonite with higher Fe contents (10 wt%) additional Fe containing species are formed.

From Mössbauer and TEM investigations it can be concluded that the calcined Fe rich aluminas contain very small  $\text{Fe}_2\text{O}_3$  particles ( $< 10$  nm).

The investigations have shown an alternative method to the coprecipitation procedure for synthesizing  $\text{Fe}_2\text{O}_3$ -containing alumina with high specific surfaces and small iron oxide particles finely divided in the  $\text{Al}_2\text{O}_3$  matrix via a crystalline precursor for  $\text{Al}_2\text{O}_3$  and further calcination. The thermal decomposition of Fe-doped dawsonites is also a suitable method for obtaining aluminas with a high percentage of well-isolated  $\text{Fe}^{3+}$  ions in lattice sites.

## Acknowledgements

The authors thank Renate Dambowsky for determining the chemical composition of the materials.

This work was supported by the German Federal Minister for Education and Science and the Berlin-State (project No. 03C 3005).

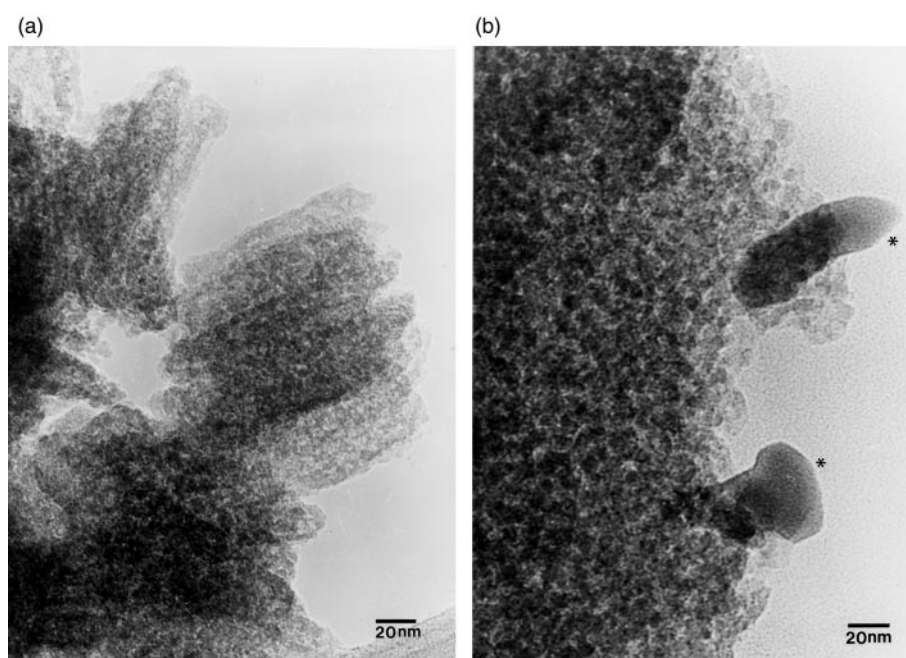


**Fig. 9** Transmission electron micrograph of samples 10A/600 (a) and 3C/600 (b), \*  $\text{Fe}_2\text{O}_3$  particles.

## References

- 1 H. Hamada, Y. Kintaichi, M. Inaba, M. Tabata, T. Yoshinari and H. Tsuchida, *Catal. Today*, 1996, **29**, 53.
- 2 S. C. Paik and J. S. Chung, *Appl. Catal. B*, 1996, **8**, 267.
- 3 Z. Suo, Y. Kou, J. Niu, W. Zhang and H. Wang, *Appl. Catal. A*, 1997, **148**, 301.
- 4 W. Ji, S. Shen, S. Li and H. Wang, *Preparation of Catalysts V*, Elsevier Science Publishers B. V., Amsterdam, 1991, p. 517.
- 5 X. Gao, J. Shen, Y. Hsia and Y. Chen, *J. Chem. Soc., Faraday Trans.*, 1993, **89**, 1079.
- 6 S. Kato, T. Iga, S. Hatano and Y. Isawa, *Yogyo-Kyokai-Shi*, 1976, **84**, 255.
- 7 J. Correia da Silva, *CA Pat.*, 2,119,312, 1994.
- 8 S. Kato, T. Iga and Y. Isawa, *Yogyo-Kyokai-Shi*, 1976, **84**, 215.
- 9 S. Brunauer, P. H. Emmet and E. Teller, *J. Am. Chem. Soc.*, 1938, **60**, 309.
- 10 E. P. Barret, L. G. Joyner and P. P. Halenda, *J. Am. Chem. Soc.*, 1951, **73**, 373.
- 11 I. Pitsch, D.-C. Uecker, D. Müller, I. Kurzawski, S. Möhmel and W. Geßner, *37th IUPAC Congress and 27th GDCh General Meeting*, Berlin, August 14–19, 1999.
- 12 K.-N. P. Kumar, J. Tranto, J. Kumar and J. E. Engell, *J. Mater. Sci. Lett.*, 1996, **15**, 266.
- 13 R. Aasa, *J. Chem. Phys.*, 1970, **52**, 3919.
- 14 G. M. Bancroft, *Mössbauer Spectroscopy*, McGraw-Hill, Maidenhead, Berkshire, England, 1973.